Proc. Natl. Acad. Sci. USA
Vol. 91, pp. 7360–7364, July 1994
Biochemistry

Energy transfer analysis of Fos–Jun dimerization and DNA binding

(transcription/fluorescence/gene regulation/oncogene)

LEKHA R. PATEL, TOM CURRAN*, AND TOM K. KERPPOLA

Roche Institute of Molecular Biology, Nutley, NJ 07110

Communicated by H. Ronald Kaback, March 28, 1994

ABSTRACT **The protooncogenes *fos* and *jun* encode proteins that bind to DNA as dimeric complexes and regulate gene expression. Protein dimerization is mediated by a leucine zipper and results in juxtaposition of regions of each protein rich in basic amino acids that comprise a bimolecular DNA binding domain. We have developed an approach based on resonance energy transfer for the quantitative analysis of dimerization and DNA binding by Fos and Jun in solution. Fos-(118–211) and Jun-(225–334) polypeptides were labeled with either 5-iodoacetamidofluorescein or rhodamine X iodoacetamide on unique cysteine residues located in their DNA binding domains. Formation of heterodimeric complexes between the labeled proteins allowed resonance energy transfer between the donor fluorescein and the acceptor rhodamine fluorophores. DNA binding induced a conformational transition that increased the efficiency of resonance energy transfer. This increase was consistent with a 3-Å reduction in the distance between the fluorophores. Using this assay, we determined the affinity of the Fos–Jun interaction and examined the kinetics of dimerization and DNA binding as well as the rate of subunit exchange. Dimerization and DNA binding by Fos and Jun were rapid, with half-times of <10 s. In the absence of DNA, Fos and Jun subunits exchanged rapidly, with a half-time of <10 s. In contrast, in the presence of DNA, the complex was extremely stable. Thus, leucine zipper-containing transcription factors may exchange subunits readily when free in solution, but not when bound to DNA.**

The initiation of gene transcription requires the assembly of multiprotein complexes in association with specific DNA sequences. A great deal has been learned recently about the proteins that are required for transcription activation and their relationship with transcription control elements (1). The structures of many individual transcription factors and transcription factor–DNA complexes have been solved using crystallography and nuclear magnetic resonance techniques (2). However, there are few approaches that allow direct analysis of the dynamics of protein complex assembly in solution. Understanding of the rate and specificity of assembly of multicomponent transcription factor complexes is essential for a full appreciation of the mechanisms responsible for the selective regulation of gene expression.

The *fos* and *jun* oncogenes have provided a useful model for the study of transcription factor interactions. Although isolated independently as retroviral transforming genes (3, 4), they encode proteins that function cooperatively in the form of a heterodimeric complex that binds to DNA and regulates transcription (5). Protein dimerization is mediated by a coiled-coil interaction involving a parallel association of leucine zipper domains (6–9). This interaction juxtaposes basic regions in each protein that form a bimolecular DNA contact surface (7, 8, 10–13). This basic region-leucine zipper (bZIP) motif is conserved among all members of the *fos* and *jun* gene families and it is shared with many other transcription factors (14). Dimerization can occur within bZIP families as well as between different groups of bZIP proteins. This multiplicity of interactions results in a complex array of protein dimers that have unique DNA binding properties (15–19).

Dimerization and DNA binding by Fos and Jun are dynamic processes that involve structural transitions in both protein and DNA. Circular dichroism analysis indicates that during heterodimer formation the Fos leucine zipper domain adopts an α-helical conformation (9, 20). Similarly, on binding to DNA, the α-helicity of the Fos and Jun basic regions is increased (20). These observations are consistent with the recently reported crystal structures of GCN4 bound to DNA (21, 22). Studies of DNA bending suggest that the DNA conformation is also changed as a consequence of the interaction with Fos and Jun (23, 24). Interestingly, different leucine zipper proteins induce distinct bends in the DNA helix (18). These findings indicate that the interaction of Fos and Jun with DNA is a dynamic process involving an induced fit between DNA and protein. To investigate this process, we developed a quantitative approach, based on resonance energy transfer, to the analysis of Fos–Jun dimerization and DNA binding in solution. The results reveal that dimerization and DNA binding are rapid processes. Although exchange of Fos–Jun subunits also occurred rapidly in the absence of DNA, there was very little exchange in the presence of DNA. Quantitation of the efficiency of energy transfer allowed determination of the distance between the two fluorophores in the presence and absence of DNA and estimation of the affinity of the Fos–Jun interaction. Thus, resonance energy transfer is a powerful approach to the analysis of transcription factor interactions.

MATERIALS AND METHODS

Protein Purification. The Fos-(139–211) and Jun-(225–334) polypeptides, as well as mutant proteins containing cysteine to serine substitutions at positions 154 and/or 204 in Fos and 272 and/or 323 in Jun or deletions of residues 139–144 in Fos or 260–266 in Jun, were overexpressed in *Escherichia coli* and purified to >95% homogeneity using nickel chelate affinity chromatography, as described (20, 25, 26). Electrophoretic gel mobility shift DNA binding assays were performed as described (26).

Preparation of Labeled Proteins. For the majority of the experiments, truncated polypeptides, Fos-(118–211) C204S and Jun-(225–334) C323S, containing unique cysteine residues were used. Proteins were labeled by incubation of 1 mg of each protein in 6 M guanidine/50 mM sodium phosphate, pH 5.5/10% glycerol/1 mM dithiothreitol (DTT) at room temperature for 30 min. Following adjustment of the pH to 8.0, 5-iodoacetamidofluorescein or rhodamine X iodoacetamide (Molecular Probes) was added to 2 mM and the reaction

The publication costs of this article were defrayed in part by page charge payment. This article must therefore be hereby marked "*advertisement*" in accordance with 18 U.S.C. §1734 solely to indicate this fact.

Abbreviation: bZIP, basic region-leucine zipper.
*To whom reprint requests should be addressed.

was incubated at room temperature for 2 h and stored overnight at 4°C. The sample was centrifuged at 30,000 × g for 30 min and the reaction was terminated by the addition of DTT to 5 mM. The labeled proteins were separated from unreacted fluorophore by two passes over NAP-10 gel filtration columns (Pharmacia) and dialyzed against several changes of 50 mM sodium phosphate, pH 7.5/10% glycerol/1 mM DTT buffer. To determine the stoichiometries of labeling, the concentrations of the labeled proteins were determined by quantitative amino acid analysis and the fluorophore concentrations were determined by absorbance spectrophotometry. A stoichiometry of 1.0 mol of fluorophore per mol of protein was routinely obtained.

Fluorescence Measurements. Fluorescence measurements were made on a Perkin–Elmer MPF-66 fluorescence spectrophotometer. The temperature was maintained at 25°C using a thermostatically controlled cell holder. All measurements were performed in 50 mM sodium phosphate (pH 7.5) containing 10% glycerol, 1 mM DTT, 5 mM $MgCl_2$, 1 mM EDTA, and 50 mM NaCl. The efficiency of energy transfer was calculated from the quenching of fluorescein emission at 530 nm. Rhodamine emission at the fluorescein emission maximum of 530 nm was negligible.

Determination of the Distance Between Fluorophores by Fluorescence Energy Transfer Analysis. The distance between two fluorophores (R) can be determined from $R = R_0(E^{-1} - 1)^{1/6}$, where E is the efficiency of nonradiative transfer and $R_0 = 9786\ (\kappa^2\ n^{-4}\ Q_D\ J)^{1/6}$ Å (27). κ^2 is a function of the relative orientations of the donor and acceptor fluorophores and the generally used value 2/3 was accepted based on the assumption of random tumbling of the fluorophores (27). The refractive index of the medium, n, was taken to be 1.4 for proteins in water. The overlap integral J (2.25×10^{-13} $cm^3 \cdot M^{-1}$) was calculated from the overlap between the Fos-F emission and Jun-R absorbance spectra (28). The donor quantum yield Q_D (0.75) was determined using disodium fluorescein in 0.1 M NaOH as a reference (27). Using these values, R_0 for Fos-F and Jun-R was calculated to be 46 Å. The calculations assume that all of the labeled molecules participate in dimerization and DNA binding, consistent with our results from Scatchard analysis.

Determination of the Dimerization Affinity of Fos–Jun by Fluorescence Energy Transfer Analysis. The efficiency of Fos-F quenching by Jun-R is directly related to the number of Fos-F/Jun-R complexes formed. The total fluorescein fluorescence is a function of the concentration and fluorescence of free Fos-F and Fos-F/Jun-R heterodimers. Thus, the concentration of Fos-F/Jun-R heterodimers can be determined as a function of the Jun-R concentration. The concentration of free Jun-R can then be calculated from the known total Jun-R concentration and the Fos-F/Jun-R heterodimer concentration. Scatchard analysis of the data was performed as described (29).

Determination of the Kinetics of Fos–Jun Association and DNA Binding. The rates of Fos–Jun association and DNA binding were determined using a Perkin–Elmer LS50B fluorescence spectrophotometer with an SFA-12 stopped-flow sample injector. The initial rates of Fos-F fluorescence quenching and the increase in Jun-R emission were estimated from time drive plots of the fluorescence. The rates of donor quenching and the increase in acceptor emission were determined in separate experiments and gave comparable results.

RESULTS AND DISCUSSION

Previously, we demonstrated that the Jun bZIP region could be labeled with fluorescein at a unique cysteine residue located in the DNA binding domain (20). The fluorescence of fluorescein-labeled Jun was enhanced by dimerization with Fos and binding to the AP-1 site. To extend these studies, we have now used fluorescence energy transfer analysis, which is based on the nonradiative transfer of quanta between donor and acceptor fluorophores, to compare the structures of Fos–Jun heterodimers in the presence and absence of DNA and to quantitate the affinity and kinetics of Fos–Jun interactions. Fluorescence energy transfer analysis is a more specific method for the study of intermolecular interactions than analysis of the fluorescence of a single fluorophore since it requires the close proximity of two fluorophores whose emission and absorption spectra overlap. Fluorescence energy transfer is also a sensitive probe of changes in protein conformation since the efficiency of energy transfer depends on the inverse sixth power of the distance between the fluorophores. The strategy used for this study is illustrated schematically in Fig. 1 *Top*. A similar approach was used previously to investigate the association of the regulatory and catalytic subunits of the cAMP-dependent protein kinase (30) and the interaction of the β subunit of DNA polymerase with the primer (28).

For quantitative application of fluorescence energy transfer analysis, it is necessary to label each protein stoichiometrically at unique sites while retaining the properties of the native proteins. Therefore, we established conditions that permitted the selective and stoichiometric labeling of unique cysteine residues in the DNA binding domains of Fos and Jun with iodoacetamide derivatives of fluorescein and rhodamine. Examples of proteins labeled with 5-iodoacetamidofluorescein, in the case of Fos (Fos-F), and rhodamine X iodoacetamide, in the case of Jun (Jun-R), are presented in Fig. 1 *Middle*. To determine the effect of labeling Fos and Jun at these sites on their dimerization activities, we compared DNA binding by labeled and unlabeled proteins using gel-shift assays at high oligonucleotide concentrations. Since dimerization is a precondition for DNA binding, any change in dimerization efficiency within the range of protein concentrations examined would result in a change in the apparent DNA binding activity. As shown in Fig. 1 *Bottom*, the DNA binding activity of Fos-F/Jun-R heterodimers was not significantly different from that of the unlabeled proteins. Thus, the labeled proteins retain the dimerization properties of unmodified Fos and Jun.

We examined energy transfer between both Jun-F and Fos-R as well as that between Fos-F and Jun-R. Energy transfer was observed between both protein combinations. However, the increase in quantum yield of Jun-F both upon dimerization with unlabeled Fos and upon binding to the AP-1 site (20) interfered with quantitation of the efficiency of energy transfer between Jun-F and Fos-R. In contrast, neither dimerization with the unlabeled proteins nor DNA binding had any effect on the fluorescence of Fos-F (data not shown). Therefore, for the quantitative analysis of Fos–Jun interactions, we used resonance energy transfer between Fos-F and Jun-R.

Emission scans were recorded between 500 and 700 nm during excitation at 490 nm of Fos-F, Fos-F with Jun-R, and Fos-F, Jun-R, and an AP-1 site oligonucleotide (Fig. 2*A*). Fos-F generated a single emission peak at the fluorescein emission maximum of 530 nm, whereas Fos-F with Jun-R yielded a reduced peak at 530 nm and increased emission at the rhodamine emission maximum of 603 nm. This reduction in fluorescein emission and the corresponding increase in rhodamine emission upon Fos-F interaction with Jun-R were caused by resonance energy transfer.

The presence of the AP-1 binding site resulted in a further decrease in the donor fluorescein emission and a corresponding increase in the acceptor rhodamine emission (Fig. 2*A*). This increase in the efficiency of energy transfer in the presence of the AP-1 site also occurred in the presence of a large excess of Jun-R. Therefore, the increase in energy transfer could not result from the formation of more Fos–Jun

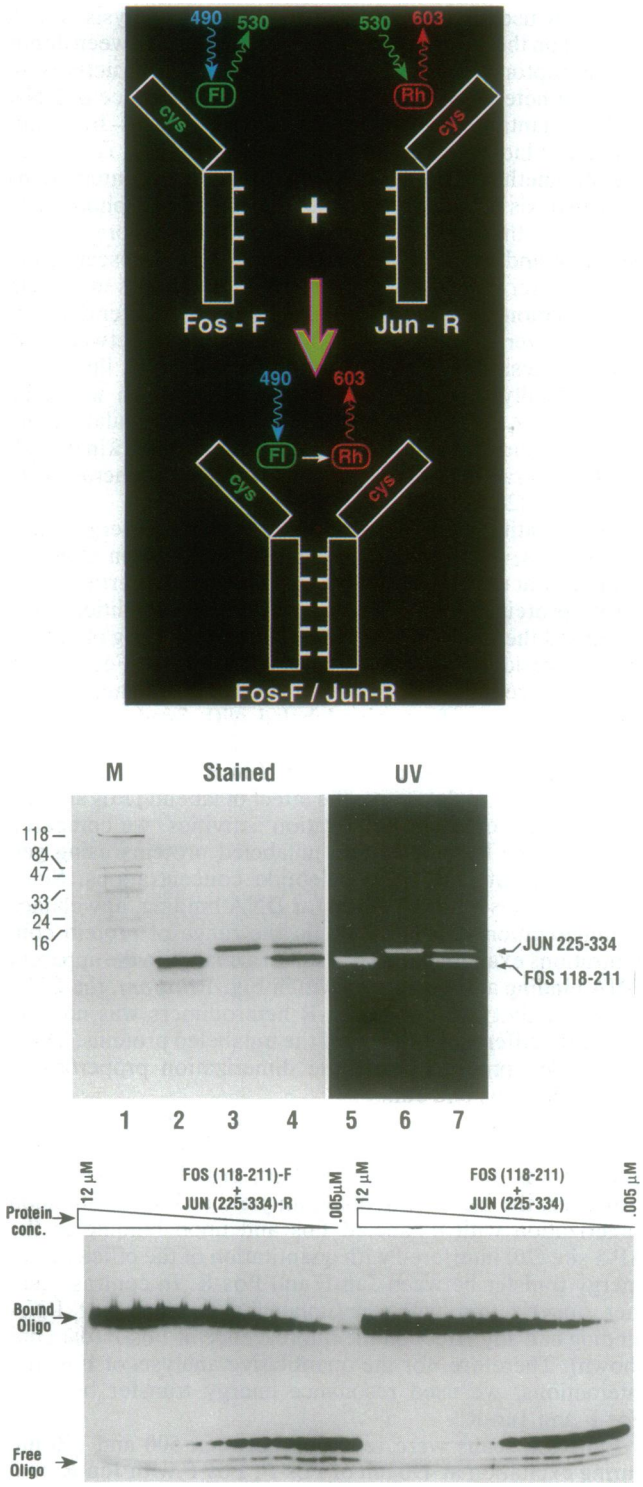

FIG. 1. (*Top*) Schematic diagram of fluorescence energy transfer between Fos-fluorescein and Jun-rhodamine. Fluorescein absorbs light at 490 nm and emits light at 530 nm. Rhodamine absorbs light at 530 nm and emits light at 603 nm. When brought in close proximity through heterodimerization mediated by the leucine zipper, light energy absorbed by fluorescein at 490 nm is transferred to rhodamine through nonradiative Förster energy transfer and emitted by rhodamine at 603 nm. (*Middle*) SDS/PAGE of Fos-F and Jun-R in parallel with the corresponding unlabeled proteins. Lane 1, molecular mass markers (in kDa; Bio-Rad); lane 2, Fos-(118–211); lane 3, Jun-(225–334); lane 4, Fos-(118–211)/Jun-(225–334); lane 5, Fos-F; lane 6, Jun-R; lane 7, Fos-F/Jun-R. Lanes 1–4 were stained with Coomassie brilliant blue and lanes 5–7 were visualized under UV light. (*Bottom*) Comparison of the DNA binding activities of Fos-F/Jun-R and unlabeled Fos-(118–211)/Jun-(225–334). Concentrations of Fos-F/Jun-R or Fos-(118–211)/Jun-(225–334) ranging from 0.005 μM to 12 μM were incubated with 0.2 μM ^{32}P-labeled AP-1 oligonucleotide. The complexes were separated on a 6.5% native polyacrylamide gel.

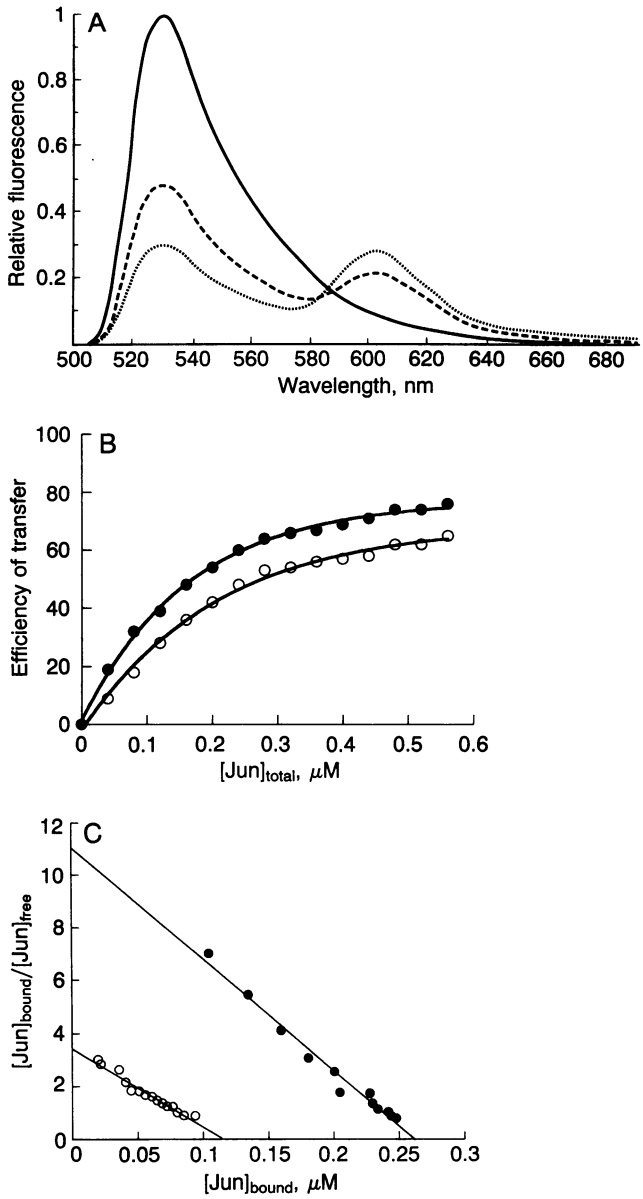

FIG. 2. (*A*) Fluorescence spectra of Fos-F (——), Fos-F with Jun-R (- - -), and Fos-F with Jun-R and DNA (· · ·). The fluorescence spectra of 0.25 μM Fos-F, 0.25 μM Fos-F with 0.5 μM Jun-R, and 0.25 μM Fos-F with 0.5 μM Jun-R and 0.2 μM AP-1 oligonucleotide were recorded between 500 and 700 nm with excitation at 490 nm. (*B*) Efficiency of Fos-F quenching as a function of total Jun-R concentration. Different amounts of Jun-R were added to 0.14 μM Fos-F and the fluorescence at 530 nm was measured in the absence (○) and presence (●) of 0.2 μM AP-1 oligonucleotide. (*C*) The data from two separate experiments in the absence of AP-1 oligonucleotide are shown in a Scatchard plot. Two different preparations of Fos-F were used, one at 0.14 μM (○) and the other at 0.28 μM (●). The plots were linear over the range between 0.02 μM and 0.25 μM of Jun-R bound. At lower Jun-R concentrations, binding was not consistent and therefore these data points were not used.

heterodimers, suggesting that binding to DNA brings the fluorophores on Fos-F and Jun-R into closer proximity, thereby increasing the efficiency of energy transfer.

These conclusions are supported by several control experiments. Denaturation of protein complexes in the presence of 3 M guanidine completely abolished energy transfer. Non-

specific DNA [poly(dI-dC) or an SP-1 oligonucleotide] had no effect on energy transfer. Energy transfer between mutated proteins lacking functional DNA binding domains was not enhanced by AP-1 oligonucleotides. Finally, energy transfer was not observed when Fos and Jun were labeled with fluorophores on C204 of Fos and C323 of Jun. Therefore, the fluorophores linked to C154 of Fos and C272 of Jun are fortuitously located to allow highly efficient and specific fluorescence energy transfer that is affected by DNA binding.

To calculate the distance between the fluorophores, we determined the efficiency of resonance energy transfer in the Fos-F/Jun-R heterodimer by extrapolation to the limit of infinite Jun-R to Fos-F ratio (Fig. 2*B*). In three independent experiments, a consistent increase in the efficiency of energy transfer was observed in the presence of DNA (E = 64% and 75%, 68% and 77%, and 64% and 74% in the absence and presence of DNA, respectively). These efficiencies correspond to estimated distances between the fluorophores of 42 Å in the absence and 39 Å in the presence of DNA. These values represent average distances over the dynamic range of each complex population. However, because of the sixth order distance dependence, they are heavily weighted toward the shortest distance between the fluorophores within each population. The 39-Å distance measured in the presence of DNA is consistent with the positions of the cysteines in Fos and Jun inferred from x-ray crystal structures for the GCN4–DNA complex (21, 22) as well as with models for the Fos–Jun–DNA complex structure derived from studies of DNA bending (23, 24). Thus, Fos and Jun undergo a conformational transition upon binding to DNA that brings the fluorophores 3 Å closer together.

Fluorescence energy transfer between Fos-F and Jun-R provides an assay for determination of the dimerization affinity in solution. Therefore, we examined the concentration dependence of Jun-R quenching of Fos-F fluorescence at several different Fos-F concentrations (Fig. 2*B*). The binding affinity, measured as the dissociation constant for the Fos-F/Jun-R interaction, was calculated from four independent experiments to be $2.3 \pm 0.9 \times 10^{-8}$ M. This calculation is based on the assumption that all of the labeled molecules participate in dimerization and that formation of Jun homodimers does not significantly compete with Fos–Jun heterodimer formation in the range of concentrations employed. The results from the Scatchard analysis are consistent with both of these assumptions (Fig. 2*C*). The dimerization affinity calculated from our experiments (2.3×10^{-8} M) was higher than that determined previously (1×10^{-7} M) using synthetic peptides in the scintillation proximity assay (31). The synthetic peptides used in those experiments spanned only the region encompassing the five leucines in the leucine zipper (31). However, the histidine residue located in phase with the leucines on the carboxyl-terminal side of the leucine zippers of Fos and Jun has been shown to be essential for efficient dimerization (32). The higher dimerization affinity measured in our experiments is consistent with a role for amino acid residues outside of the heptad repeat of leucine residues in determining dimerization affinity. Alternatively, differences in experimental conditions between our studies and those reported previously (31) may have contributed to the difference in dimerization affinities measured.

Since fluorescence energy transfer analysis allows monitoring of real-time changes in fluorophore interactions, it can be used to analyze the kinetics of protein–protein and protein–DNA association, dissociation, and exchange. Therefore, we attempted to determine the rates of heterodimer formation, subunit exchange, and DNA binding using Fos-F and Jun-R. These rates were measured from the initial rates of change in both donor and acceptor fluorescence following sample mixing. The rate of heterodimer formation was fast, with a half-time of <10 s (Fig. 3*A*). The rate of DNA binding

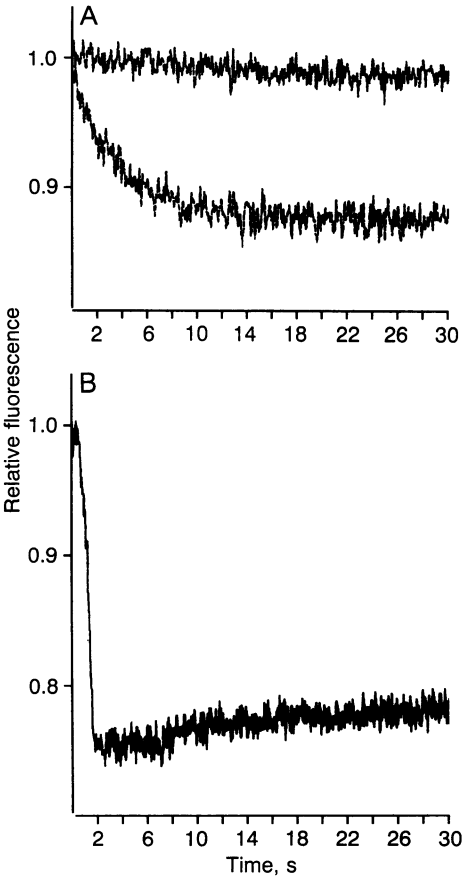

FIG. 3. (*A*) Kinetics of Fos-F/Jun-R heterodimerization. Equal volumes of 0.5 μM Fos-F and 1 μM Jun-R (lower trace) or 0.5 μM Fos-F and storage buffer (upper trace) were mixed using an SFA-12 stopped-flow injector and the time-dependent quenching of fluorescein emission at 530 nm was plotted. The fluorescence was normalized to the initial value at time 0. (*B*) Kinetics of Fos-F/Jun-R binding to DNA. Fos-F/Jun-R heterodimers formed by preincubating 0.5 μM Fos-F with 1 μM Jun-R were mixed with an equal volume of 0.4 μM AP-1 oligonucleotides using an SFA-12 stopped-flow injector and the time-dependent quenching of fluorescein emission at 530 nm was plotted. The fluorescence was normalized to the initial value at time 0.

was even faster, with a half-time of <5 s (Fig. 3*B*). The half-times of these reactions varied with the experimental conditions but were faster than 15 s under all conditions tested. These results indicate that the conformational transition that occurs upon Fos and Jun binding to the AP-1 site is a rapid event that may occur concomitant with DNA binding. This conformational transition may therefore contribute to the specific recognition of the AP-1 site. We have shown previously that many bZIP proteins can induce a change in the structure of the AP-1 site, which may contribute to its specific recognition (18). This change in DNA structure may be coupled to a conformational transition in the proteins that bind to this site. Further studies of the interaction between Fos, Jun, and DNA will be necessary to elucidate the dynamics of this flexible protein–DNA complex.

To follow the rate of subunit exchange, the time dependence of the decrease in acceptor fluorescence following the addition of a 10-fold excess of unlabeled Fos was measured (Fig. 4*A*). The rate of exchange in the absence of DNA was rapid, and the complex half-life was <10 s at 25°C. However, in the presence of an excess of specific DNA only 15% of the complex exchanged over a period of 16 h. To confirm the results from energy transfer analysis, we also followed the exchange reaction using a gel-shift assay (Fig. 4*B*). Fos-

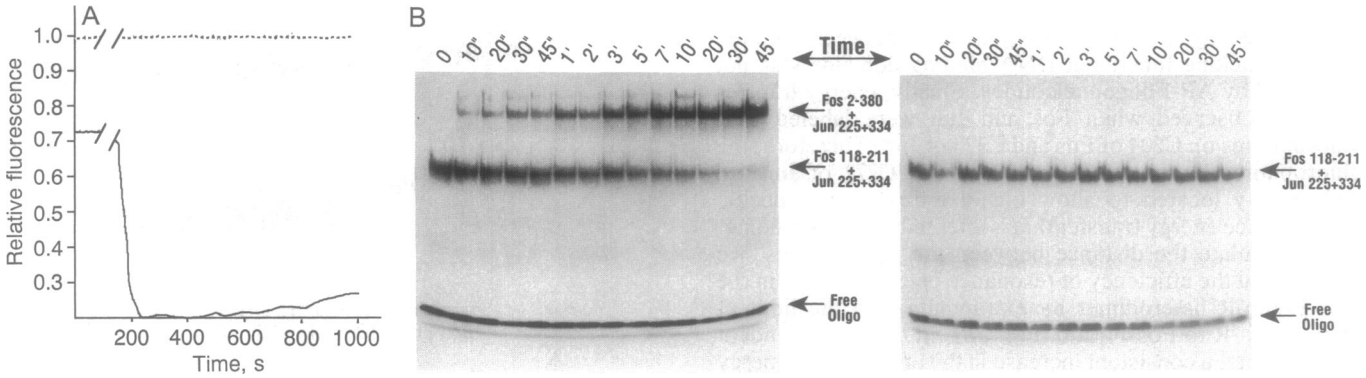

FIG. 4. (*A*) Analysis of the exchange of Fos and Jun in the presence and absence of DNA by fluorescence energy transfer. Fos-F and Jun-R (0.25 μM each) were allowed to equilibrate in the absence (· · ·) or presence (——) of 0.2 μM AP-1 oligonucleotide at 25°C. Unlabeled Fos was added to 2.5 μM and the acceptor fluorescence at 530 nm was monitored. The curves are broken at the times the cuvette was removed to allow sample addition and mixing. The half-time of exchange was estimated from the initial slope of the plot. The fluorescence was normalized to the initial value of Fos–Jun heterodimers in the presence of the AP-1 site. (*B*) Analysis of the exchange of Fos and Jun by electrophoretic mobility shift analysis. Fos-(118–211) and Jun-(225–334) (0.064 μM each) were incubated for 30 min at 37°C, followed by an additional 15 min of incubation in the absence (*Left*) or presence (*Right*) of 0.2 μM ^{32}P-labeled AP-1 oligonucleotide at 25°C. At time 0, full-length Fos was added to 0.95 μM and the samples were incubated at 25°C. At the times indicated above the lanes, the reaction mixtures were transferred to ice and 0.2 μM ^{32}P-labeled AP-1 oligonucleotide was added to the samples incubated in the absence of DNA. The complexes were separated on a 6.5% native polyacrylamide gel at 4°C.

(118–211) and Jun-(225–334) were mixed in equimolar concentrations and allowed to dimerize. Subsequently, a 20-fold excess of full-length Fos was added in the presence or the absence of AP-1 binding sites. The gel-shift assay is not well suited for the analysis of rapid exchange processes because of the time required for loading and running the gel. However, using either labeled or unlabeled proteins, Fos and Jun were found to exchange rapidly in the absence but not in the presence of DNA. Thus, specific DNA binding traps Fos–Jun heterodimers in a conformational state that does not allow subunit exchange. This effect is specific for the AP-1 site since an SP-1 oligonucleotide did not alter the rate of subunit exchange. Our experiments have been performed *in vitro* under defined conditions, and, since the conditions *in vivo* are not known, it is not possible to predict definitively the properties of these complexes *in vivo*. However, our results suggest that bZIP complexes may freely exchange subunits in the absence of a DNA target sequence but may not exchange when specifically bound to DNA.

Fos and Jun do not function in isolation to effect their regulatory roles. They interact with many other transcription factors that can modify or mediate their functions. Some of these interactions, such as that with the glucocorticoid receptor, can occur in the absence of DNA (33), whereas others, such as that with NFATp, occur when bound to DNA (34, 35). Transcription activation by many transcription factors has been proposed to be mediated through contacts with general initiation factors or other proteins associated with the transcription initiation complex. However, despite the likely importance of many of these interactions, little is known about their affinities or kinetics. Additional studies using quantitative methods for the analysis of protein–protein and protein–DNA interactions in solution will be necessary to evaluate the affinity and specificity of these events. Our studies to date using the Fos–Jun model system demonstrate that fluorescence energy transfer analysis is a powerful tool that allows determination of structural, thermodynamic, and kinetic parameters of macromolecular interactions.

We thank Mark Greip, Roger Tsien, and Jonathan Lee for helpful discussions and Sidney Udenfriend, Nathan Nelson, and Steve Blacklow for critical reading of the manuscript.

1. McKnight, S. L. & Yamamoto, K. R., eds. (1992) *Transcriptional Regulation* (Cold Spring Harbor Lab. Press, Plainview, NY).
2. Harrison, S. C. (1991) *Nature (London)* **353**, 715–719.
3. Curran, T. & Teich, N. M. (1982) *J. Virol.* **42**, 114–122.
4. Maki, Y., Bos, T. J., Davis, C., Starbuck, M. & Vogt, P. K. (1987) *Proc. Natl. Acad. Sci. USA* **84**, 2848–2852.
5. Curran, T. & Franza, B. R., Jr. (1988) *Cell* **55**, 395–397.
6. Landschulz, W. H., Johnson, P. F. & McKnight, S. L. (1988) *Science* **240**, 1759–1764.
7. Gentz, R., Rauscher, F. J., III, Abate, C. & Curran, T. (1989) *Science* **243**, 1695–1699.
8. Turner, R. & Tjian, R. (1989) *Science* **243**, 1689–1694.
9. O'Shea, E. K., Rutkowski, R., Stafford, W. F., III, & Kim, P. S. (1989) *Science* **245**, 646–648.
10. Vinson, C. R., Sigler, P. B. & McKnight, S. L. (1989) *Science* **246**, 911–916.
11. Abate, C., Luk, D. & Curran, T. (1990) *Cell Growth Differ.* **1**, 455–462.
12. O'Neil, K. T., Hoess, R. H. & DeGrado, W. F. (1990) *Science* **249**, 774–778.
13. O'Shea, E. K., Rutkowski, R. & Kim, P. S. (1992) *Cell* **68**, 699–708.
14. Kerppola, T. & Curran, T. (1991) *Curr. Opin. Struct. Biol.* **1**, 71–79.
15. Macgregor, P. F., Abate, C. & Curran, T. (1990) *Oncogene* **5**, 451–458.
16. Hai, T. & Curran, T. (1991) *Proc. Natl. Acad. Sci. USA* **88**, 3720–3724.
17. Hoeffler, J. P., Lustbader, J. W. & Chen, C.-Y. (1991) *Mol. Endocrinol.* **5**, 256–266.
18. Kerppola, T. & Curran, T. (1993) *Mol. Cell. Biol.* **13**, 5479–5489.
19. Kerppola, T. K. & Curran, T. (1994) *Oncogene* **9**, 675–684.
20. Patel, L., Abate, C. & Curran, T. (1990) *Nature (London)* **347**, 572–575.
21. Ellenberger, T. E., Brandt, C. J., Struhl, K. & Harrison, S. C. (1992) *Cell* **71**, 1223–1237.
22. König, P. & Richmond, T. J. (1993) *J. Mol. Biol.* **233**, 139–154.
23. Kerppola, T. & Curran, T. (1991) *Cell* **66**, 317–326.
24. Kerppola, T. K. & Curran, T. (1991) *Science* **254**, 1210–1214.
25. Abate, C., Luk, D., Gentz, R., Rauscher, F. J., III, & Curran, T. (1990) *Proc. Natl. Acad. Sci. USA* **87**, 1032–1036.
26. Abate, C., Patel, L., Rauscher, F. J., III, & Curran, T. (1990) *Science* **249**, 1157–1161.
27. Lakowicz, J. R. (1983) *Principles of Fluorescence Spectroscopy* (Plenum, New York).
28. Greip, M. A. & McHenry, C. S. (1992) *J. Biol. Chem.* **267**, 3052–3059.
29. Scatchard, G. (1949) *Ann. N.Y. Acad. Sci.* **51**, 660.
30. Adams, S. R., Harootunian, A. T., Buechler, Y. J., Taylor, S. & Tsien, R. Y. (1991) *Nature (London)* **349**, 694–697.
31. Pernelle, C., Frédéric Clerc, F., Dureuil, C., Bracco, L. & Tocque, B. (1993) *Biochemistry* **32**, 11682–11687.
32. Cohen, D. R. & Curran, T. (1990) *Oncogene* **5**, 929–939.
33. Kerppola, T. K., Luk, D. & Curran, T. (1993) *Mol. Cell. Biol.* **13**, 3782–3791.
34. Jain, J., McCaffrey, P. G., Miner, Z., Kerppola, T., Lambert, J. N., Verdine, G. L., Curran, T. & Rao, A. (1993) *Nature (London)* **365**, 352–355.
35. McCaffrey, P. G., Luo, C., Kerppola, T., Jain, J., Badalian, T., Ho, A., Burgeon, E., Lane, W. S., Lambert, J. N., Curran, T., Verdine, G. L., Rao, A. & Hogan, P. G. (1993) *Science* **262**, 750–754.